Cryomilling for the Fabrication of a Particulate B_4C Reinforced Al Nanocomposite: Part I. Effects of Process Conditions on Structure

JICHUN YE, JIANHONG HE, and JULIE M. SCHOENUNG

Metal matrix composites (MMCs) are a relatively new category of engineering materials, which provide tailorable properties to meet specific needs. Cryomilling, mechanical milling at cryogenic temperatures, was employed in this study to fabricate nanostructured metal matrix composite powder with nanocrystalline aluminum alloys as the matrix and particulate B_4C as the reinforcement. Cryomilling provided an extremely low temperature for the processing of this composite, which prevented the formation of secondary phases that are detrimental to mechanical properties. A uniform distribution of B_4C in the Al and a clean strong interface between them were achieved. The contamination that results from cryomilling was analyzed. The effects of the B_4C addition and the process control agent (PCA) on the microstructure of the composite powder were investigated. Results indicate that these additives had significant, yet opposing, effects on powder yield; a slight effect on contamination, particle size, and particle morphology; and no detectable effect on grain size refinement in the matrix.

I. INTRODUCTION

METAL matrix composites (MMCs) are a type of advanced material with a metal matrix reinforced with other stronger materials (normally ceramics) in the form of continuous fibers, short fibers, whiskers, or particles. Early studies focused on fiber-reinforced composites,[1] but it was soon demonstrated that the high cost of continuous fibers and the complicated fabrication routes constrained the applications to very limited areas, such as for the aerospace industry. Thereafter, research gradually became refocused on discontinuous reinforcements, due to lower cost, ease of fabrication, isotropic properties, and reasonable improvement in properties. Although any metallic alloy system can be used for the matrix, much of the MMC research and development activity has been concentrated on aluminum alloys because of their low densities. Aluminum alloys reinforced with particulate ceramics can offer a range of property enhancements over monolithic alloys, *e.g.,* higher strength and stiffness, improved high-temperature properties, better wear resistance, and lower thermal expansion.[2] The properties of aluminum matrix composites can be easily tailored by appropriate selection of the aluminum alloys and the reinforcements with an appropriate volume fraction.

Various aluminum matrix composite systems with reinforcing phases of B_4C,[3–13] SiC,[2,9,11,12] Al_2O_3,[2,10,14] BN,[15] and AlN[16] have been developed *via* various techniques. Covalently bonded solids based on B, C, or N form the hardest materials, and B_4C ranks the third just after diamond and cubic boron nitride.[17] In addition, B_4C has a lower specific gravity of 2.51 g/cm^3 (less than that of aluminum, 2.7 g/cm^3), compared to 3.21 g/cm^3 for SiC, 3.51 g/cm^3 for diamond, and 3.92 g/cm^3 for Al_2O_3.[17] These unique properties, along with other attractive properties[18] such as high impact and wear resistance, high melting point, good resistance to chemical agents, and high capacity for neutron absorption, make B_4C a likely candidate as the reinforcement in an Al matrix composite.[3–13] Fabrication of dense Al/B_4C materials using liquid phase approaches is difficult, however, because a temperature as high as 1100 °C is needed for the Al to completely wet the B_4C surface,[3,5,8] and processing at such high temperatures leads to the formation of a series of high-temperature phases from chemical reactions between the B_4C and the Al.[3–8] Powder metallurgy processing is another approach to manufacturing Al/B_4C composites.[3,19–21] The blended Al/B_4C powders, after being degassed, are compacted by cold isostatic pressing,[19] hot isostatic pressing (HIPing),[20,21] or dynamic powder compaction.[13] These compacts are subsequently processed using hot working methods such as extrusion, forging, and rolling.[19,20,21] The composites fabricated by powder metallurgy methods normally have weak interfaces between the ceramic and the metal. These interfaces tend to debond when exposed to an applied load, resulting in a deterioration in mechanical behavior.[21]

Mechanical milling has produced notable improvements in the strength, toughness, fatigue life, and corrosion resistance of aluminum alloys.[22,23,24] The success of prior work in fabricating high-performance aluminum alloys by mechanical milling leads to the logical next step of using mechanical milling to intentionally incorporate hard ceramics, thereby producing metal matrix composites with superior mechanical performance. Previous studies have shown that mechanical milling can be used to fabricate Al matrix composites.[25,26] However, in these studies, the process had a different purpose than for normal mechanical milling. The purposes of the milling, instead, were effectively to mix the reinforcements with the matrix and to enfold the matrix material around each reinforcing particle,

JICHUN YE, Senior Process Development Engineer, is with Spansion Inc. JIANHONG HE, Principal Scientist, is with Research & Development, Osram Sylvania, Twanda, PA 18848. JULIE M. SCHOENUNG, Professor, is with the Department of Chemical Engineering and Materials Science, University of California, Davis, CA 95616-5294. Contact e-mail: jmschoenung@ucdavis.edu

Manuscript submitted October 21, 2005.

which would eliminate the voids between the Al alloy and the SiC reinforcement and achieve solid-state bonding between them. The microstructure of the Al matrix was not taken into consideration. Thus, the milling time used was much shorter than that used with normal mechanical milling.

In addition to the effects already described, mechanical milling, especially the variation called cryomilling, is capable of producing a nanocrystalline grain structure in the matrix, resulting in a greatly improved strength due to the finer grain size.[27,28] Cryomilling, which is mechanical milling at cryogenic temperatures, takes advantage of both the extremely low temperature of the liquid nitrogen medium and the positive attributes associated with conventional mechanical milling. The temperature rise during milling is an unavoidable problem in conventional mechanical milling, resulting in severe recovery and recrystallization of fine microstructures.[24] The extremely low milling temperature in cryomilling suppresses the recovery and recrystallization and leads to finer grain structures and more rapid grain refinement.[24] Potential chemical reactions between the reinforcement and the matrix are also suppressed at such a low temperature. In addition, when aluminum and aluminum alloys are cryomilled, 2- to 10-nm sized aluminum nitride and oxy-nitride particles form, which results in improved strength and thermal stability of these materials even after high-temperature consolidation.[23,24,29] Cryomilling, as a newly developed milling technique, is one of the few techniques available to produce nanostructured metallic powder in large quantities[30] and has the potential to be economically feasible.[31]

During mechanical milling, high toughness powders, such as Al alloy powders, stick on the balls, shaft, and wall of the tank.[32] To avoid severe sticking, a process control agent (PCA) should be used, such as stearic acid [$CH_3(CH_2)_{16}CO_2H$]. This agent suppresses the cold welding that occurs between the powder particles and between the powder particles and the milling media. The particle size of the milled powder can also be modified by the amount of stearic acid used in the mechanical milling.[32] Another problem associated with mechanical milling is powder contamination. The contamination sources include the milling tools, milling atmosphere, and PCA. Chemical composition, especially the impurity concentration in the cryomilled powder, should be understood clearly, because these impurities will affect the microstructural evolution (such as grain growth) during consolidation and the mechanical properties of the consolidated materials.[23,24,29]

In this study, Al matrix composite powders were successfully fabricated using cryomilling, with the goal to combine the following potential advantages: (1) the uniform incorporation of hard reinforcements, (2) the strong bonding between B_4C and Al, (3) the presence of nanostructure in the Al matrix, (4) the presence of extremely fine nitride and oxy-nitride particles, (5) the absence of the chemical reaction between B_4C and Al, and (6) the capability of mass production. This in-depth study on the powder is important for a deep understanding and ultimate control of the subsequent consolidation process, as well as to explain the mechanical behavior obtained in the consolidated material.[33,34] The objectives of the current study are sixfold: (1) to fabricate composite Al/B_4C powders with a nanocrystalline matrix using cryomilling, (2) to evaluate the distribution of the reinforcement in the matrix, (3) to characterize the reinforcement-matrix interface, (4) to investigate the effect of the B_4C on the microstructure of the composite powder, (5) to reveal the effect of PCA on the microstructure of the composite powder, and (6) to study the powder yield for cryomilling.

II. EXPERIMENTAL PROCEDURE

A. *Materials*

Composite powders consisting of particulate B_4C reinforcement (submicron-to-several micron) in nanocrystalline Al matrices (either pure Al or 5083 Al alloy) were fabricated using the cryomilling technique. The starting Al alloys were elemental Al powder (99 wt pct Al, particle size < 40 μm, Alfa Products, Danvers, MA) or 5083 Al alloy powder (Al: 94.7, Mg: 4.4, Mn: 0.7, and Cr: 0.15 wt pct, particle size < 44 μm, Valimet Inc., Stockton, CA), both of which are inert gas-atomized powders with spherical shape. The B_4C powder (Wacker Engineered Ceramics, Inc., Adrian, MI) was faceted with the particle size of 1 to 7 μm and 2 to 14 μm for F1200 and F800, respectively. F1200 and F800 B_4C powders have the same chemical composition (B: 78.3, C: 19.5, and O: 1.0 wt pct). The Al (and the 5083 Al) powder was blended with either F800 or F1200 B_4C and stearic acid in the ratios designated in Table I, using a V-blender.

B. *Cryomilling*

In the current study, 0.2, 0.5, and 1 wt pct stearic acid was used. The resulting mixture was cryomilled for 8 hours in a Union Process 1-S (Union Process, Inc., Akron, OH) attritor mill. The balls used for milling were made of stainless steel (AIAI 440-C, Cr: 16 to 18, C: 1.0 to 1.2, Mg: <1.0, Si <1.0 wt pct, balance Fe), 0.635 cm in diameter, and were added at a ball-to-powder ratio of 32:1 (mass basis). The drive shaft was operated at a speed of 180 rpm. A thermocouple was positioned at a specific height at which it just contacted the top surface of the liquid

Table I. Cryomilling of (B_4C + Al/5083 Al), 180 rpm, 8 h, and Stainless Steel Balls

Powder Label*	Matrix	Particle Size of B_4C	Stearic Acid (wt pct)	B_4C (wt pct)
AS05-10	Al	1–7 μm	0.5	10
AS10-10	Al	1–7 μm	1.0	10
5L02-10	5083	2–14 μm	0.2	10
5L10-10	5083	2–14 μm	1.0	10
5S10-10	5083	1–7 μm	1.0	10
5S02-00	5083	NA	0.2	0
5S02-10	5083	1–7 μm	0.2	10
5S02-15	5083	1–7 μm	0.2	15
5S02-20	5083	1–7 μm	0.2	20
5S02-25	5083	1–7 μm	0.2	25

*The first digit: "A" represents Al and digit "5" represents 5083 Al alloy; the second digit: "S" stands for B_4C with a particle size of 1–7 μm and "L" stands for B_4C with a particle size of 2–14 μm. The next two digits designate the amout of stearic acid (in x.x wt pct), and the final two digits designate the amount of B_4C in the mixture (in wt pct).

nitrogen. The measured temperature was maintained at −180 °C ± 5 °C. The change in the measured temperature was used as an indicator of the need to adjust the flow of the liquid nitrogen to maintain the level of liquid nitrogen in the milling tank and ensure complete immersion of the powder and milling balls.

C. *Powder Characterization*

On the basis of the ASTM E1019 and ASTM E1097 standards, chemical analysis of the as-received and cryomilled powders was conducted by Luvak Inc. (Boylston, MA). The morphology of the cryomilled powders and the distribution of the reinforcement within the powders were examined with a PHILIPS* XL 30 scanning electron microscope (SEM). The milled powders were glued using epoxy and polished to prepare the cross sections for the SEM analysis. Particle size and size distribution of the milled powders were evaluated with a Coulter LS100Q particle analyzer. X-ray diffraction (XRD) measurements were performed using Cu K_α radiation in a Siemens D5000 diffractometer (New York, NY) equipped with a graphite monochromator. A low scanning rate of 0.12 deg/min was used to ensure the accuracy of the measurements. The peak position and full-width at half-maximum (FWHM) of the XRD reflections, computed using a software package available with the Siemens D5000 diffractometer, were used to calculate the average grain size in the cryomilled powders. The measured profile is a convolution of the instrumental broadening profile and the intrinsic broadening profile. Subtraction of the influence of the instrumental broadening was made on the basis of an assumption regarding the shapes of the intrinsic profile and the instrumental profile (the profile from an annealed sample).[35,36] Also, the intrinsic broadening has two components, grain size broadening, and microstrain broadening, which can be separated by using some well-established methods.[35,36] Transmission electron microscopy (TEM) studies were completed with a PHILIPS CM 20 microscope operated at 200 keV, and the TEM samples were prepared using the following procedure.[28] The powders and epoxy were mixed to create a slurry, which was then mounted into a stainless steel nut, sliced from a stainless steel pipe with an outside diameter of 3 mm and an inside diameter of 2 mm, to form a 3-mm diameter disk. The disk was ground and then dimpled to approximately 30-μm thickness using a dimpler fitted with alumina grinders. The particle size of the alumina grinders descended from a 3-μm grade down to a 1-μm grade. The final thinning perforation process was carried out using a Gatan 600 argon ion mill (Gatan Inc., Pleasanton, CA) at the temperature of near liquid nitrogen temperature (the extension of the sample holder was soaked in liquid nitrogen) with an angle range from 22 to 10 deg.

*PHILIPS is a trademark of Philips Electronic Instruments Corp., Mahwah, NJ.

III. RESULTS

A. *Chemical Composition*

The results of the chemical composition analysis for selected powders are listed in Table II. For comparison purposes, the nominal contents of B and C that result directly from the B_4C phase itself were calculated and are also incorporated in Table II.

Table II. Chemical Composition of Cryomilled Powders (wt pct)

Powder Label	Fe	C	O	N	B
As-received B_4C (F1200)	0.2	19.5	1.0	1.0	78.3
As-received 5083 Al	0.35	0.02	0.29	<0.001	0.049
5S02-00	0.57	0.18	0.70	0.40	0.053
5L02-10 (nominal)	0.95	2.24 (2.17)	0.98	0.54	6.29 (7.80)
5S02-10 (nominal)	0.88	2.26 (2.17)	1.37	0.62	6.90 (7.80)

The results show that cryomilling leads to noticeable contamination. The Fe contamination is from the wear of the stainless steel milling tank, shaft, arms, and balls during cryomilling, which was more severe for the powders containing hard particles. The presence of the hard B_4C results in higher contamination of Fe, C, O, and N. Apparently, a larger B_4C particle leads to more Fe contamination, similar C contamination, but less O and N contamination, when compared to composite powders cryomilled with smaller B_4C particles. The Fe contamination is greater when the B_4C particles are larger because the larger hard particles caused more severe wear of the milling tank, shaft, arms, and balls.

Interpretation of the C content of the cryomilled powders is less straightforward than for the Fe content. Cryomilling alone increased the C content from 0.02 to 0.18 wt pct as the result of the use of stearic acid (which, it should be noted, would normally be removed by degassing prior to consolidation), as well as the potential contamination from the stainless steel milling media. Based on the calculation for the Fe contamination, the potential for contamination of C from the stainless steel has been determined to be negligible. If the nominal C content (derived from the B_4C content) is subtracted from the measured values, the C contamination levels are 0.07 and 0.09 wt pct for the 5L02-10 and 5S02-10 powders, respectively, which is much less than the value of 0.18 wt pct in the cryomilled 5083 Al without B_4C (5S02-00). However, note that the B content after cryomilling was lower than the nominal content, indicating that some B_4C particles may have been lost during cryomilling. If the lower B content value is used as the basis for calculating the nominal C content, these latter values calculate to be 1.8 to 1.9 wt pct. Consequently, the C contamination is then 0.36 and 0.44 wt pct for the 5S02-10 and 5L02-10 samples, respectively. Therefore, the presence of B_4C particles leads to an increase in C contamination in the matrix primarily because of the preferential adsorption of the stearic acid onto the B_4C particles.

The milling atmosphere is the source of the O and N contamination. Exposure of the powders to air, especially during powder collection after cryomilling when cryoadsorption is severe, should be minimized to ensure a minimum level of contamination of O. Another O source may be the liquid nitrogen, because of insufficient separation of liquid oxygen and liquid nitrogen. The O contamination from stearic acid is calculated to be negligibly

small. Nitrogen is picked up during cryomilling because cryomilling is carried out in liquid nitrogen. In order to clarify the effect of B_4C on the N and O contamination, four sources of contamination must be considered: pickup by the aluminum during milling, pickup by the B_4C during milling, pickup by the starting powder before milling, and any direct contribution from the stearic acid. Pickup by the Al during cryomilling is based on the N and O contamination of the 5083 Al powder without B_4C (5S02-00), while the O contamination from the stearic acid is only 0.02 wt pct and can be neglected. As shown in Table II, the as-received B_4C has a higher N and O content than the as-received 5083 Al. By subtracting the N and O from the as-received powders (Al alloys and B_4C) and the N and O pickup by the Al during cryomilling, the net increase in N content due to the pickup by the B_4C during cryomilling is 0.08 and 0.16 wt pct for 5L02-10 and 5S02-10, respectively; while the net increase in O content due to the pickup by the B_4C during cryomilling is 0.25 and 0.64 wt pct for 5L02-10 and 5S02-10, respectively. It is interesting to note that the O contamination is greater than the N contamination when B_4C is present, whereas they are approximately equal (0.4 wt pct) for the cryomilled 5083 Al without B_4C. Although the average particle sizes for the 5S02-00, 5L02-10, and 5S02-10 powders are similar in value, the surfaces of the composite powders are rougher[28] and have more surface area, leading to the increase in N and O contamination. The smaller B_4C particles in sample 5S02-10, having a larger area of interface between the B_4C particles and the matrix, facilitate the pickup of N and O. Thus, O can be adsorbed at these interfaces, as well as at external surfaces and crevices. It should be noted that alumina was not detected in any of the powders by either X-ray diffraction or electron diffraction in TEM.

B. *Powder Morphology and Size*

The cryomilled 5083 Al powder (5S02-00) has a chunk morphology (Figure 1(a)), which is similar to the morphology observed for cryomilled Ni powders[28] and mechanically milled Al and Mg powders.[37] Figure 1(b) shows the morphology of the cryomilled composite powders, indicating a similar morphology as for the cryomilled monolithic Al. Careful examination of the cryomilled powder surface at higher magnification (not shown) revealed that the surface of the composite powder is rougher than that of the monolithic Al. In a related study, the morphology of the cryomilled powder particles was observed to switch from thick chunk to a rougher particle by introducing 2 wt pct of hard particles into a Ni matrix.[28]

In the current study, the cryomilled composite powders with 1 wt pct stearic acid (5L10-10 and 5S10-10) have much smaller particle sizes with narrower size distributions compared to those with 0.2 wt pct stearic acid (5L02-10 and 5S02-10), as shown in Table III. The weight percent of reinforcement (from 10 to 25 wt pct) has no significant influence on the morphology of the cryomilled composite powders, but affects the particle size and size distribution, as shown in Table III. Both the average particle size and the size distribution decrease when more B_4C is added. Moreover, as seen from the data in Table III, it is apparent that the starting size of B_4C particles does not affect the final composite particle size.

C. *Grain Size and Microstrain in the Al Matrix*

It is well established that cryomilling can produce powders with a grain size in the nanometer regime and that the grain size and microstrain can be estimated by analyzing the broadening of XRD peaks.[29,38] Figure 2 depicts a

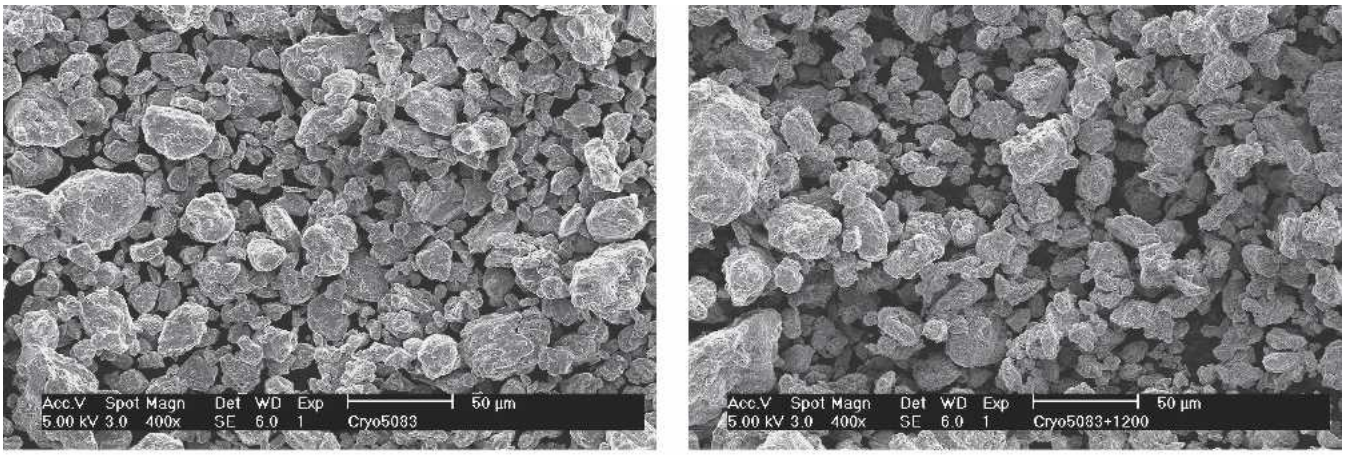

Fig. 1—The morphology of the cryomilled powder: (*a*) cryomilled 5083 Al powder sample (5S02-00), showing a thick chunk morphology; and (*b*) cryomilled 5083 Al/B_4C composite powder sample (5S02-10), showing a similar morphology as cryomilled monolithic 5083 Al.

Table III. Average Particle Sizes of the Cryomilled Powders, Measured with the Coulter Particle Analyzer

Powder Label	5L02-10	5L10-10	5S10-10	5S02-00	5S02-10	5S02-15	5S02-20	5S02-25
Average particle size (μm)	59.76 ± 48.44	16.39 ± 14.02	13.36 ± 10.16	60.40 ± 46.59	58.69 ± 46.59	51.50 ± 41.31	45.47 ± 37.04	47.91 ± 34.84

typical XRD spectrum for the cryomilled composite powders, on the basis of which grain size and microstrain of the matrix for an individual sample are feasibly calculated using established methods.[35,36] However, because the intensity of the reflections from the B_4C is relatively low compared to that of the 5083 Al, the calculation for grain size and microstrain of B_4C particles is not practical.

The equation $\beta \cos \theta = k\lambda/D + 16e^2 \sin^2 \theta/\beta \cos \theta$ was used to calculate the grain size and microstrian of the cryomilled aluminum matrix, where $k = 1$, λ is the wavelength (in the case of Cu $K_{\alpha 1}$, $\lambda = 0.15406$ nm), θ *is* the diffraction angle, D is the grain size, and β is the FWHM.[35,36] If $\beta \cos \theta$ is plotted against $\sin^2 \theta/\beta \cos \theta$ for several XRD reflections, the data should be on a straight line, with a slope of $16e^2$ and an intercept of $k\lambda/D$. The resulting grain size and microstrain values for the cryomilled powders were calculated and are listed in Table IV. It can be seen that a relatively invariant grain size of 24 to 27 nm and microstrain of approximately 0.2 pct were obtained, regardless of the material composition and amount of stearic acid used for cryomilling.

D. *Distribution of B_4C in the Al Matrix*

A uniform distribution of B_4C particles in the aluminum matrix is crucial to achieve composites with good mechanical properties. To demonstrate the distribution of the B_4C particles in the Al matrix, a cross section of sample 5S02-10 was prepared and examined by SEM in backscattered mode. Figure 3(a) is an image at low magnification, indicating a uniform distribution of B_4C particles in both small and large composite particles. This homogeneous distribution was also confirmed with optical microscopy (not shown). Figure 3(b) is an image at higher magnification of the largest composite particle in Figure 3(a). Figure 3(c) is a detailed view of the interior of this same particle. B_4C particles are capable of ''penetrating'' all matrix particles to form a uniform distribution in the matrix. It is worth noting that only a few B_4C particles are observed on the surface of the cryomilled particles and most of the B_4C particles are distributed within the Al matrix (Figure 3). B_4C particle size was measured using SEM (statistically from 200 B_4C particles), which indicates that the B_4C particle size decreased slightly during cryomilling. As shown in Figure 3(c), the B_4C particle size was reduced to a size of 1.2 ± 0.6 μm compared to 1 to 7 μm in the as-received F1200 B_4C powder. The angular shape of the B_4C particles was retained after 8 hours of cryomilling. Segregation of the reinforcement phase was not observed.

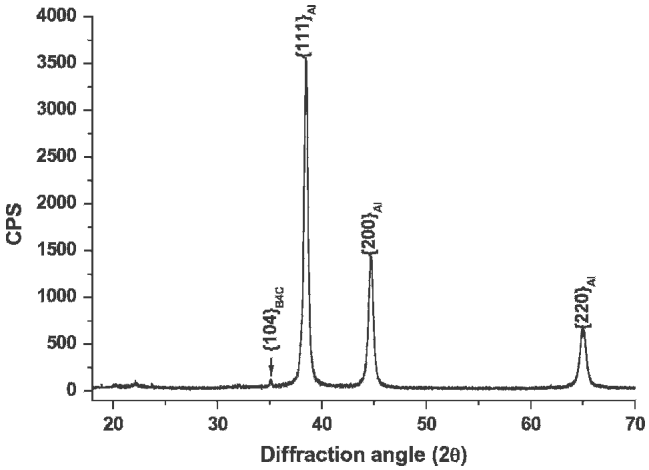

Fig. 2—XRD spectrum for the cryomilled Al/B_4C composite powder (sample 5S02-10), indicating a low intensity reflection from the B_4C reinforcement.

Table IV. Grain Size and Microstrain for the Cryomilled Powders

Powder Label	Matrix	B_4C (wt pct)	Matrix Grain Size (nm)	Strain (%)	Correlation Coefficient
AS05-10	Al	10	27.3	0.190	0.85
AS10-10	Al	10	26.0	0.197	0.94
5L02-10	5083	10	24.1	0.201	0.85
5L10-10	5083	10	24.3	0.205	0.86
5S10-10	5083	10	24.5	0.201	0.91
5S02-00	5083	0	25.5	0.205	0.89
5S02-10	5083	10	24.4	0.199	0.94
5S02-15	5083	15	24.4	0.200	0.95
5S02-20	5083	20	24.4	0.206	0.92
5S02-25	5083	25	24.5	0.207	0.87

E. *TEM Studies on the Microstructure*

The TEM results for samples AS05-10 and 5S02-10 indicate that, in both samples, the matrix has a nanocrystalline structure with an average grain size of approximately 30 nm (29 ± 15 nm for sample AS05-10 and 27 ± 14 nm for sample 5S02-10, which were statistically measured from 300 Al grains in the dark-field TEM images), which is a little larger than the average grain sizes determined from XRD calculations (Table IV). Individual grains with sizes approaching 60 nm were occasionally observed in the matrix. Figure 4 shows low-magnification TEM images of sample AS05-10, indicating a composite powder that consists of a nanocrystalline Al matrix and coarse B_4C particles. Consistent with the results from SEM, Figure 4 shows the B_4C particles to be homogenously distributed in the nanocrystalline Al matrix; no clustering has occurred. Figure 5(a) is a detailed view of the B_4C particle in the lower-right corner in Figure 4(b). Figure 5(b) is a higher magnification of the area indicated by the arrow in Figure 5(a). There are no voids or cracks between the matrix and the B_4C particle, which indicates that cryomilling, unlike other MMC processing methods, does not result in a weak matrix-reinforcement interface. Such a weak interface would be detrimental to the mechanical performance. Figure 5(c) shows a selected area diffraction (SAD) pattern at the interface of the B_4C particle and the matrix (the area indicated by the arrow in Figure 5(a)) and the corresponding index. The diffraction pattern is composed of polycrystalline rings from fcc Al and spots from the B_4C particle. The uniform ring pattern from the Al indicates that the nanocrystalline Al grains are randomly orientated. Secondary phases that have typically appeared at high temperature, such as $AlB_{24}C_4$, Al_4BC, Al_4C_3, and AlB_2,[5,6] were not detected in the present powder mixture. Figure 5(d) is a dark-field image taken at $g = [003]_{B4C}$, indicating the B_4C particle alone. The boundary of the B_4C particle is relatively rough, which may be caused by the impact and

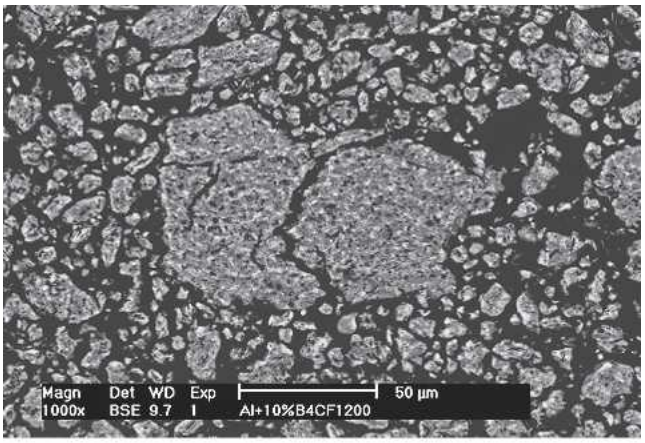

(*a*)

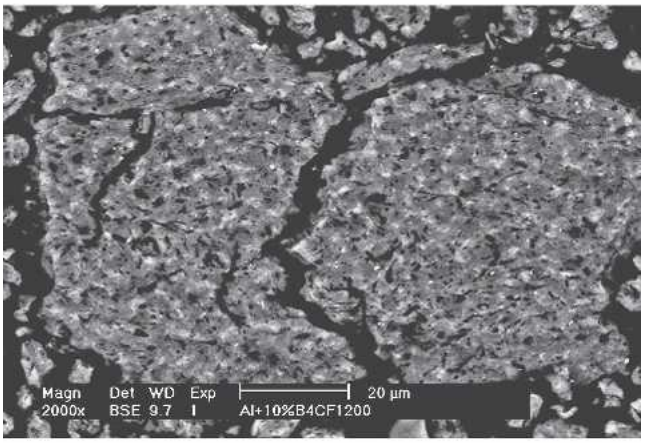

(*b*)

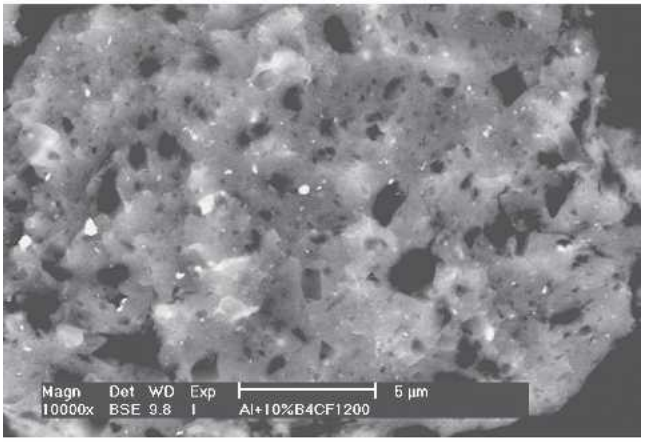

(*c*)

Fig. 3—SEM images (BSE) on a cross section of the cryomilled 5083 Al/B_4C composite powder (sample 5S02-10). The black spots in the images are B_4C particles. The white spots are Al_2O_3 particles from the alumina grinding media used during sample polishing. (*a*) SEM image on a cross section of the cryomilled Al/B_4C composite powder, indicating a uniform distribution of B_4C particles in the Al matrix in sample 5S02-10; (*b*) higher magnification of (a); and (*c*) a detailed view of the interior of a particle of the cryomilled Al/B_4C composite powder, indicating that the B_4C particle size is in the range of 0.2 to 2 μm.

friction during cryomilling. A rough boundary is beneficial to cohesion. Figure 5(e) is a dark-field image taken at $g = [1\text{–}13]_{B4C}$ and $\{111\}_{Al}$, which allows the configuration of the B_4C particle and the matrix to be observed. Furthermore, this image also confirms that the grain size of the matrix is consistent with the value determined with XRD.

F. *Powder Yield*

Powder yield here refers to the weight fraction of powder recovered from the milling chamber after cryomilling is completed. High powder yield for the cryomilled composite powder is desired in order to reduce the processing cost, and thus the final product cost. Many factors, such as processing procedures and materials composition, can affect the powder yield for cryomilling. Empirically, a small increase in the amount of processing control agent improves yield greatly, although the usage of PCA should be minimized to avoid degradation of properties after consolidation. As shown in Figure 6(a), without a PCA, only 10 wt pct of the composite powder was collected after cryomilling, due to the severe adhesion of Al onto the milling tools. Addition of 0.2 and 1.0 wt pct stearic acid resulted in higher powder yields of 70 and 90 wt pct, respectively. The stearic acid, as a PCA, should be used for ductile materials during cryomilling to prevent severe adhesion and improve the powder yield. From this point of view, it is expected that with a higher fraction of hard B_4C, *i.e.,* a smaller fraction of ductile aluminum, less stearic acid will be necessary, or the powder yield should improve for a given amount of stearic acid. However, the opposite is observed. The yield decreases linearly with increasing amount of the hard B_4C particles, as shown in Figure 6(b). The possible explanation is that the stearic acid is more likely to be adsorbed at the B_4C-Al interfaces, so that the effective amount of stearic acid available for the Al is small.

IV. DISCUSSION

A. *Contamination*

Koch[39] pointed out two potentially serious problems associated with mechanical milling: (1) contamination from the milling media and atmosphere and (2) grain coarsening during consolidation. The contamination problem sometimes excludes mechanical milling as a feasible processing method, if a material with high purity is necessary for certain special applications. Special design and selection of materials for milling tools might be necessary to minimize the contamination. For example, applying a coating with the same chemical composition as the powders being milled onto the milling tools, or a coating that is more resistant to wear, or using more wear resistant milling balls will reduce the contamination.[24] Such special designs will result in higher processing cost for cryomilling and are appropriate only for those applications with strict compositional requirements. The hardness of the powders being milled will also affect the level of contamination. There will be more metallic contamination (*e.g.,* Fe) with harder milled powders. For example, the cryomilling of a Ni-based alloy[40] led to more Fe contamination than an Al-based alloy (5S02-00). Likewise, the presence of hard particles

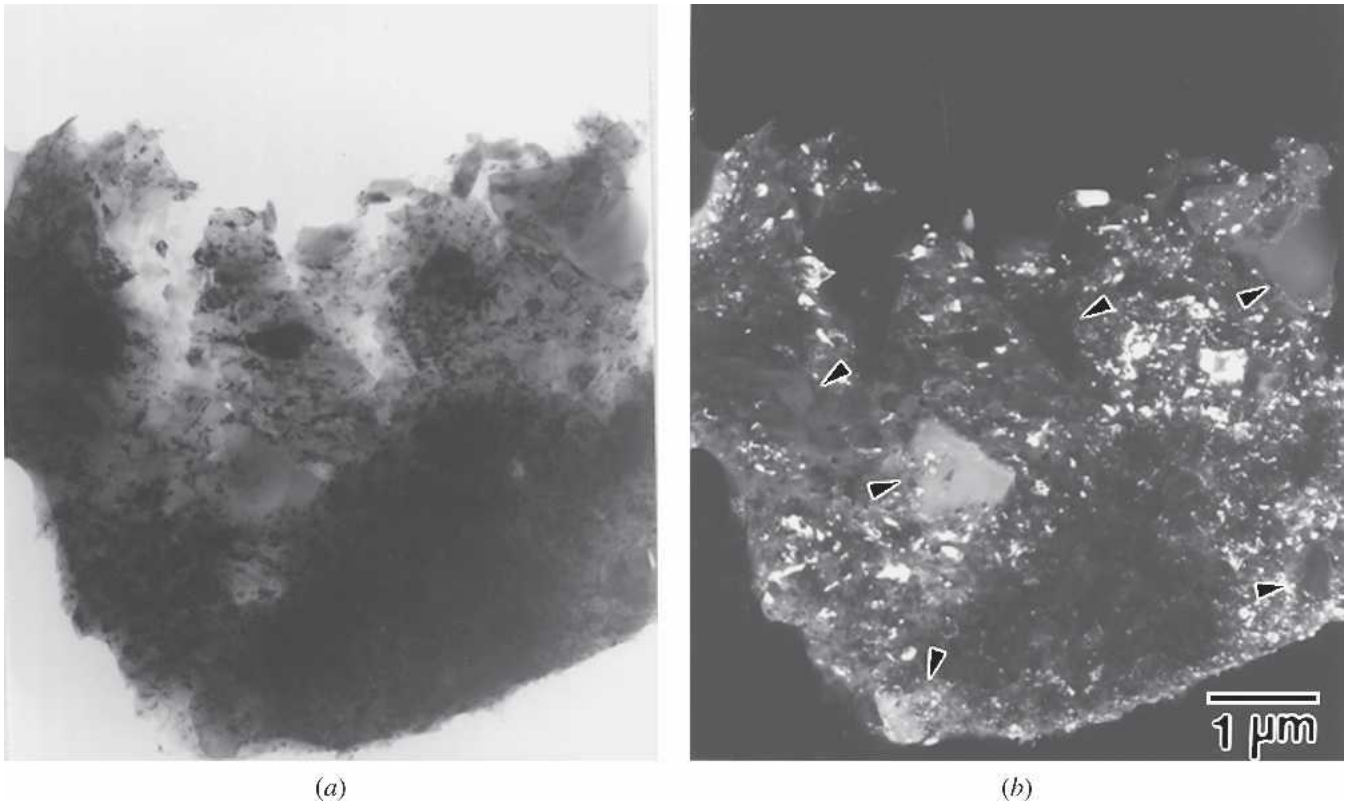

Fig. 4—Low-magnification TEM images of cryomilled Al/B_4C composite powder (sample AS05-10). Arrows indicate boron carbide particles, which are in the size range from submicron to micron: (*a*) bright-field image and (*b*) dark-field image.

(such as B_4C) will result in higher Fe contamination, as was observed in the current study (Table II).

It is worth noting that the contamination from cryomilling does not necessarily degrade the properties of the milled materials, but can instead enhance the strength and thermal stability, as described in Section I. The presence of B_4C particles leads to more significant contamination (Table II), which can result in a material that is more thermally stable. For example, sample 5S02-10 retained an average grain size of 41 nm after degassing at 400 °C for 24 hours, which provides a good indication that the consolidated material would also have an ultra-fine microstructure and good mechanical properties.

B. *Effect of Process Control Agent*

Since mechanical milling is a process of repeated cold welding and fracturing, a balance between them should be reached to achieve successful mechanical milling. However, this balance may not be achieved in most cases by mechanical milling itself, especially for soft materials.[24,37] For example, only 10 wt pct of the Al composite powder (Figure 6(a)) was collected after cryomilling due to the severe adhesion of Al (*i.e.,* the dominant cold-welding process). In order to achieve a balance between fracturing and welding, a PCA, acting as a surfactant, is needed for mechanical milling of Al.[24,37] Stearic acid is one of the most effective PCAs and is widely used in mechanical milling. Normally, for the conventional mechanical milling of soft metals, such as Mg and Al, 1 to 3 wt pct of stearic acid is used.[37] A higher concentration of stearic acid in the milling system will suppress the excessive cold welding, resulting in an improved powder yield (Figure 6(a)). In the current study, it was found that for cryomilling of 5083 Al, the addition of only 0.2 wt pct of stearic acid led to a 90 wt pct powder yield after 8 hours of cryomilling (Figure 6(b)), which is comparable to the powder yield for Al in conventional mechanical milling with 1 wt pct of stearic acid for the same milling time,[37] indicating that cryomilling results in the need for less stearic acid. For cryomilling, the extremely low temperature can modify the deformation mode of the powder, making fracture easier. Furthermore, the liquid nitrogen used during cryomilling also acts as a surfactant, reducing the surface energy of each freshly fractured surface. Therefore, less stearic acid is necessary for cryomilling compared to that required in conventional mechanical milling. Although stearic acid can improve the powder yield, a minimum amount should be used, because it also introduces some additional contaminants, such as C, H, and O. These elements might not be completely removed by the subsequent degassing process, resulting in the degradation of mechanical behavior. The C in stearic acid can form some phases such as Al_4C_3.[22,24,41] From this point of view, as little stearic acid as possible should be used for mechanical milling. On the other hand, more stearic acid can improve the powder yield (Figure 6(a)), which will reduce the processing cost.[31] A trade-off should be made between these two effects to achieve high powder yield, as well as to ensure high-quality properties. In our material system, as shown in Figure 6(a),

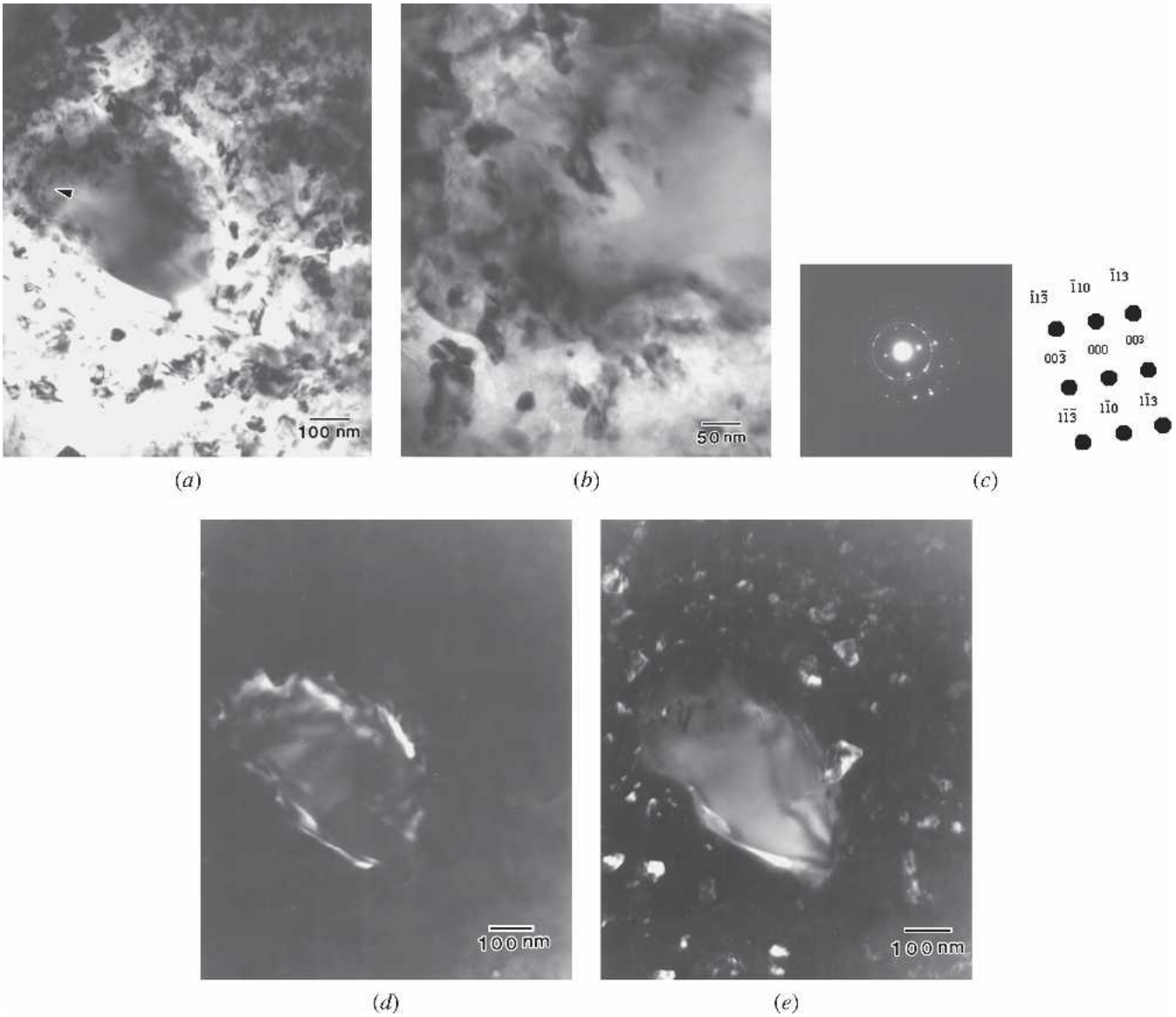

Fig. 5—High-magnification TEM images of the cryomilled Al/B_4C composite powder. (*a*) A detailed view of the lower-right corner of Fig. 4(b), indicating a small B_4C particle in the Al matrix; (*b*) the interface between the Al matrix and the B_4C particle, identified by the arrow in (a), within the cryomilled Al/B_4C composite powder; (*c*) selected electron diffraction pattern from the Al/B_4C interface shown in (b) (in the cryomilled Al/B_4C composite powder), $B = [3\text{-}30]_{B4C}$; (*d*) TEM dark-field image of the B_4C particle in the cryomilled Al/B_4C composite powder taken by $g = [003]_{B4C}$; and (*e*) dark-field image taken by $g = [1\text{–}13]_{B4C} + \{111\}_{Al}$, highlighting both the B_4C particle and the matrix grains in the cryomilled Al/B_4C composite powder.

the use of more than 1 wt pct stearic acid has little impact on the powder yield and is, therefore, not recommended.

The particle size of milled powders can be important for subsequent consolidation processes. For example, a specific particle size of milled powders is required as a feedstock powder in thermal spray or cold spray, making sieving of the milled powder a necessary step.[28] The particle size of the milled powders can be adjusted by controlling the amount of stearic acid used.[32] The amount of stearic acid needed is a function of the composition of the powder, the milling time, and the desired particle size of milled powder. For a given composition and milling time, there is a direct relationship between the amount of stearic acid used and the desired particle size.[32] As indicated in Table III in the current study, it was observed that the use of more stearic acid resulted in a decrease in the average particle size of the milled powder and a narrower particle size distribution. This ability to control particle size by controlling the stearic acid content can provide the opportunity to minimize the need for sieving.

C. *Effect of B_4C on the Microstructure*

B_4C is a hard ceramic material different from ductile aluminum. Powders with different weight fractions of B_4C powder (F1200) (from 0 to 25 pct) were cryomilled under identical milling conditions to investigate the effect of the B_4C particles on the microstructure and particle morphology. As shown in Table III, both the average particle size and the breadth of the particle size distribution decreased as the weight fraction of B_4C particles increased, indicating that the B_4C particles have a similar effect as a

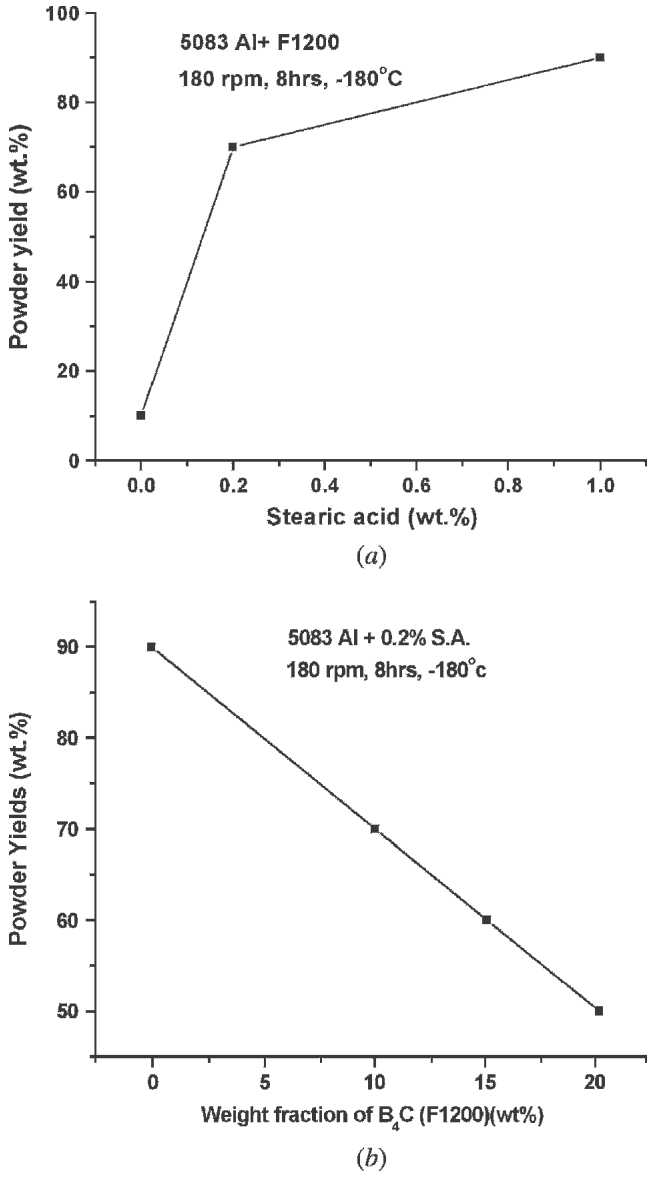

Fig. 6—Variation in powder yield of cryomilled composite powders with variations in stearic acid and B_4C content: (*a*) powder yield *vs* amount of stearic acid and (*b*) powder yield *vs* weight fraction of B_4C.

process control agent in modifying these parameters. However, the PCA and B_4C additions result in an opposite effect on powder yield, as observed in Figure 6. The B_4C particles are more apt to adsorb stearic acid than are the Al particles, due to their smaller size and larger surface area, thus reducing the effectiveness of the stearic acid. The implication of this result is that the B_4C particles do not act as a surfactant, as the stearic acid does. Instead, the observed effect of B_4C on particle size, *i.e.,* that the average particle size and particle size distribution decreased as the B_4C concentration increased, can be rationalized on the basis of an effect on the fracture mode. With the presence of the B_4C particles, the surface of the powder after milling was rougher (Figure 1) and more crevices were observed near the B_4C particles (not shown), indicating that the presence of the B_4C particles can facilitate the fracture process, leading to a smaller particle size for the composite powder. The starting size of the B_4C particles seems to have no apparent influence on the final composite particle size. This can be rationalized by the fact that the two B_4C powders are not significantly different in particle size (F1200 (1 to 7 μm) and F800 (2 to 14 μm).

A relatively invariant grain size of 25 nm for the Al matrix, regardless of the type of Al, the weight fraction of B_4C particles (0 to 25 pct), and the addition of process control agent (0.2 to 1 wt pct), as shown in Table IV, support the conclusion that the existence of B_4C particles in the Al alloy does not influence the final grain size for the nanostructured Al matrix. In a related study, Chung *et al.* found that a small introduction of AlN particles with an initial size of 2 μm into Ni facilitated the grain refinement process for Ni during cryomilling, greatly reducing the Ni grain size from 132 nm for pure Ni to 65 nm and 37 nm for Ni with 0.5 and 2.0 wt pct AlN, respectively, after milling for 8 hours.[38] During cryomilling, the AlN particles broke into nanoscaled particles, from 2 μm to 20 to 300 nm. This enhancement in the grain refinement process for the Ni matrix was interpreted on the basis of a mechanism involving the interactions of dislocations with fractured small hard particles, and the thermally induced dislocation generation due to the difference in thermal expansion coefficient between matrix and reinforcement.[38] Since cryomilling is conducted under liquid nitrogen atmosphere, the temperature variation is minimal and the dislocation generation due to the mismatch of the thermal expansion coefficient can be neglected. In the current study, the change in size of the B_4C particles was small, from 1 to 7 μm to 0.2 to 2 μm. These fractured B_4C particles are not small enough to provide sufficient interaction with dislocations, *i.e.,* to act as a source of dislocations. The grain size refinement of the Al matrix is related to the dislocation activity, which is discussed in detail in Part II of this series of articles.[42] It should also be taken into consideration, as discussed previously, that the presence of the B_4C particles during cryomilling resulted in an increase in contamination (C, O, and N) and that these elements may exist in the form of tiny dispersoids.[29,40] However, the difference in contamination levels between the Al with and without B_4C is not very significant. Therefore, the extra introduction of these tiny dispersoids, which resulted from the presence of the B_4C particles, has a limited influence on the facilitation of the grain refinement in Al during cryomilling. Since the B_4C particles do not interact with dislocations and do not result in more dislocations, the presence of the B_4C particles does not affect the formation of the nanocrystalline structure in the Al matrix, as evidenced by the Al grain sizes in the milled particles with various compositions (Table IV).

D. *The Interface between Al and B_4C*

The quality of the interface between a matrix and a reinforcement determines the performance of the consolidated composite material. The strength of the interface determines the failure modes and mechanical properties of the composite.[43] A strong interface allows for effective load transfer from the matrix to the reinforcement, leading to improved strength and stiffness. If the interface bonding is not strong enough, interface debonding will occur when the composite is subjected to an applied load.

Various liquid-phase methods for fabricating Al/B_4C composites require high temperatures to completely wet the B_4C surface and achieve a good particle-matrix interface.[3,5,8] Processing at such high temperatures leads to the formation of a series of high-temperature phases ($AlB_{24}C_4$, Al_4BC, Al_4C_3, and AlB_2) that result from the chemical reactions between Al and B_4C,[3–8] and has been systematically investigated by Pyzik *et al.*[4,5] The presence of these reaction products is detrimental to the mechanical properties.[4,5] Viala *et al.*[6] determined that as long as the Al was in the solid state, namely, the temperature was lower than 660 °C, the chemical reactions proceeded very slowly. They determined that only Al and B_4C were in a sample that was heated to 650 °C and held for 160 hours.[6] In contrast, the temperature during cryomilling is very low (−180 °C). Therefore, the formation of these reaction products is not expected during cryomilling, nor is it actually observed in the XRD spectrum (Figure 2) or in the TEM SAD pattern (Figure 5(c)). Moreover, the secondary phases also will not form during subsequent consolidation steps, because all of these steps take place at temperatures below 525 °C.[33,34] Therefore, cryomilling and the subsequent consolidation steps can produce clean interfaces, free of the high-temperature phases, between the Al matrix and the B_4C reinforcement.

Cryomilling not only provides an opportunity for low-temperature processing of metal matrix composites to prevent the formation of secondary phases, but also produces a strong solid-state bond between the reinforcement and the matrix, potentially as a result of the cold welding process that occurs during cryomilling. Jatkar *et al.*[25] used mechanical milling to enfold the matrix material around each reinforcing particle to provide a good bond between the matrix and the reinforcement. In another related study by Upit *et al.*,[44] cold welding in vacuum was used to form a strong bond between the freshly cleaved surfaces of Si or Ge (covalently bonded, elemental semiconductor materials) with sheets of Al, Pb, and In (metals). These bonds were determined to be even stronger than those within the metals, as subsequent failure did not occur at the interface, but instead through the metal. During cryomilling, repeated fracturing and cold welding occurs between metallic particles.[24,37] One consequence of this is the continuous generation of fresh metallic surfaces. Although it has not been demonstrated in the current study that the covalently bonded B_4C can be directly cold welded to the Al matrix, the similarity between this system and those in the Upit *et al.* study provide an indication that the cold welding that occurs between metals during cryomilling could also be the source of the strong interface between the matrix metal and the (covalent) ceramic reinforcement. Evidence of the strong interface, though somewhat indirect, is provided in a fractographic study by Ye *et al.*,[33] on a bulk composite made from the cryomilled composite powder in the current study. This study showed that only a few B_4C particles were observed on the fracture surface, which is far less than the 10 wt pct as intentionally introduced, indicating that the interface debonding is not a dominant failure mechanism and that the bonding between the Al and the B_4C is strong. This observation can also be supported by the fact that only a few B_4C particles were observed on the surfaces of the cryomilled Al/B_4C particles (observed in a higher magnification SEM image of Figure 1(b), not shown) and most of the B_4C particles are distributed within the Al matrix (Figure 3), because these surfaces were produced as a result of fracturing during cryomilling. A detailed investigation of the distribution of the B_4C particles is provided in Part II of this series of articles.[42] The greatly improved strength (~1000 MPa) of the bulk composite material fabricated by cryomilling and subsequent consolidation has been attributed primarily to this clean strong interface that developed during cryomilling, which leads to a more effective load transfer from the matrix to the reinforcement.[34] It should be noted that, although the material was deformed during consolidation (*i.e.,* extrusion), the severity of the strain during cryomilling would have been significantly greater than that experienced during the extrusion, which had a reduction ratio of only 6.5:1.[34] Therefore, the cryomilling would have the greatest influence on the strength of the interface. In contrast, Zhang *et al.*[21] investigated a bulk Al/B_4C composite fabricated with conventional powder metallurgy methods (blending plus extrusion or hipping), and demonstrated that extensive interface debonding occurred during mechanical testing, indicating weak bonding between the reinforcement and matrix. In conclusion, cryomilling can, potentially through cold welding, form a clean and strong interface between the reinforcement and the matrix, making the load transfer more effective.

E. *Distribution of the B_4C in the Al Matrix*

The use of cryomilling not only forms a clean and strong matrix/reinforcement interface, it also provides a more homogeneous mix than can be achieved *via* conventional blending.[20,24,25] A homogeneous distribution of the reinforcement is required to achieve a composite with good performance. Prasad *et al.*[45] investigated the relationship between the homogenization of the reinforcement in the matrix and the tensile properties. It was observed that the more homogeneously distributed composites resulted in a higher yield strength as well as a higher elongation, due to the more homogeneous deformation in the matrix and more effective load transfer from the matrix to the reinforcement. Not all matrix/reinforcement systems can be fabricated into homogenous, high-performance composites using blending, especially when the particle size of the reinforcement becomes smaller. For instance, Zhang *et al.*[46] developed an Al/mullite composite in which the mullite particles agglomerated. The mullite agglomerates made it difficult to achieve a fully dense material using hipping, which degraded the mechanical properties.[46] Similar issues occur in the liquid-phase processes, such as in casting. As an alternate technique, mechanical milling can produce metal matrix composites with a homogeneous distribution of reinforcement in the matrix, even when the size of the reinforcement is in the nanometer region. As shown in Figure 3, the B_4C particles are uniformly distributed in the Al matrix as a result of the repeated process of fracturing and cold welding. The mechanisms through which the uniform distribution is achieved are discussed in Part II of this series of articles.[42] As another example, diamond particles with a size of 4 to 5 nm were introduced into an Al-Mg alloy by cryomilling and a composite with homogeneously distributed diamond particles was achieved.[47] It is clear that mechanical milling is capable of creating a uniform

distribution of the reinforcement in the metal matrix, even when the size of the reinforcement is very small. This is one of the advantages of mechanical milling over other methods for distribution.

V. CONCLUSIONS

Composite powders of boron carbide in a matrix of nanocrystalline aluminum or 5083 Al alloy were successfully fabricated. The main results are briefly summarized as follows.

1. The Al matrix had an average grain size of 24 to 30 nm, according to measurements by X-ray diffraction and transmission electron microscopy.
2. The B_4C particles experienced a slight reduction in size and were uniformly distributed in the Al matrix; no segregation or agglomeration was observed.
3. A clean strong interface between the B_4C particle and the matrix was formed as a result of the cryomilling process; no voids or cracks were observed around the interfaces; and high-temperature phases that result from conventional processing, such as Al_3BC, AlB_2, $Al_3B_{48}C_2$, $AlB_{24}C_4$ and Al_4C_3, which are detrimental to mechanical properties, were not observed in the composite powders fabricated *via* cryomilling.
4. The experimental conditions, including the chemical composition of the matrix, the initial particle size of the B_4C (1 to 7 or 2 to 14 μm), and the weight fraction of the B_4C (from 10 to 25 wt pct), had no detectable influence on the grain size evolution in the matrix of the fabricated composite particles. The presence of B_4C particles led to a rougher surface on the composite powder particle, but had a negligible influence on the ultimate degree of grain refinement in the Al matrix.
5. The amount of stearic acid added as a process control agent affected the average particle size of the cryomilled powders, as well as the powder yield.

ACKNOWLEDGMENT

Financial support was provided by the Office of Naval Research under Contract No. N00014-03-C-0164.

REFERENCES

1. D.K. Hale: *J. Mater. Sci.*, 1976, vol. 11, pp. 2105-41.
2. D.J. Lloyd: *Int. Mater. Rev.*, 1994, vol. 39, pp. 1-23.
3. D.C. Halverson, A.J. Pyzik, I.A. Aksay, and W.E. Snowden: *J. Am. Ceram. Soc.*, 1989, vol. 72, pp. 775-80.
4. B.S. Lee and S. Kang: *Mater. Chem. Phys.*, 2001, vol. 67, pp. 249-55.
5. A.J. Pyzik and D.R. Beaman: *J. Am. Ceram. Soc.*, 1995, vol. 78, pp. 305-12.
6. J.C. Viala, J. Bouix, G. Gonzalez, and C. Esnouf: *J. Mater. Sci.*, 1997, vol. 32, pp. 4559-73.
7. K.B. Lee, H.S. Sim, S.Y. Cho, and H. Kwon: *Mater. Sci. Eng., A*, 2001, vol. A302, pp. 227-34.
8. A.J. Pyzik and I.A. Aksay: *Processing of Ceramics and Metal Matrix Composites,* Proc. Int. Symp., Pergamon Press, Elmsford, NY, 1989, pp. 269-80.
9. K.B. Lee, H.S. Sim, S.Y. Cho, and H. Kwon: *Metall. Mater. Trans. A*, 2001, vol. 32A, pp. 2142-47.
10. M. Kouzeli and A. Mortensen: *Acta Mater.*, 2002, vol. 50, pp. 39-51.
11. R.U. Vaidya, S.G. Song, and A.K. Zurek: *Phil. Mag. A*, 1994, vol. 70, pp. 819-36.
12. J.P. Lucas, J.J. Stephens, and F.A. Greulich: *Mater. Sci. Eng., A*, 1991, vol. A131, pp. 221-30.
13. G.M. Bond and O.T. Inal: *Comp. Eng.*, 1995, vol. 5, pp. 9-16.
14. A. Daoud and W. Reif: *J. Mater. Proc. Technol.*, 2002, vol. 123, pp. 313-18.
15. K.B. Lee, H.S. Sim, S.W. Heo, H.R. Yoo, S.Y. Cho, and H. Kwon: *Compos. Part A*, 2002, vol. 33, pp. 709-15.
16. M. Naranjo, J.A. Rodriguez, and E.J. Herrera: *Scripta Mater.*, 2003, vol. 49, pp. 65-69.
17. P.T.B. Shaffer: *in Engineered Materials Handbook,* M.M. Gauthier, ed., ASM INTERNATIONAL, Materials Park, OH, 1991, vol. 4, pp. 804-1002.
18. F. Thevenot: *Key Eng. Mater. (Adv. Ceram.)*, 1991, vols. 56–57, pp. 59-88.
19. R.A. Carden: *Sintered Metal-Matrix Composites Manufactured with Boron Carbide Doped for Improved Bonding*, Alyn Corporation, Irvine, CA, 1996, application no. US 94-183728.
20. A.R. Begg and A.D. Tarrant: *Preparation of Composites*, British Petroleum Co., London, United Kingdom, 1988, application no. US 4749545.
21. H. Zhang, M.W. Chen, K.T. Ramesh, J. Ye, J.M. Schoenung, and E.S.C. Chin: *Mater. Sci. Eng. A*, in press.
22. J.H. Weber and R.D. Schelleng: *Dispersion Strengthened Aluminum Alloys*, TMS, Warrendale, PA, 1998, pp. 467-82.
23. V.L. Tellkamp, A. Melmed, and E.J. Lavernia: *Metall. Mater. Trans. A*, 2001, vol. 32A, pp. 2335-43.
24. C. Suryanarayana: *Progr. Mater. Sci.*, 2001, vol. 46, pp. 1-184.
25. A.D. Jatkar, R.D. Schelleng, and A.J. Varall, Jr.: *Process for Producing Composite Materials*, MPD Technology Corp., WV, 1986, application no. US 4623388.
26. M.S. Zedalis and P.S. Gilman: *Aluminum-Based Metal Matrix Composites from Mechanically Alloyed Powder*, Allied-Signal, Inc., NJ, 1990, application no. WO 4946500.
27. C. Goujon, P. Goeuriot, M. Chedru, J. Vicens, J.L. Chermant, F. Bernard, J.C. Niepce, P. Verdier, and Y. Larrent: *Powder Technol.*, 1999, vol. 105, pp. 328-36.
28. J. He and J.M. Schoenung: *Metall. Mater. Trans. A*, 2003, vol. 34A, pp. 673-83.
29. F. Zhou, J. Lee, S. Dallek, and E.J. Lavernia: *J. Mater. Res.*, 2001, vol. 16, pp. 3451-58.
30. D.G. Morris: *Mechanical Behaviour of Nanostructured Materials*, Trans Tech Publications, Uetikon-Zuerich, Switzerland, 1998.
31. J. Ye and J.M. Schoenung: *Adv. Eng. Mater.*, 2004, vol. 6, pp. 656-64.
32. Y.F. Zhang, L. Lü, and S.M. Yap: *J. Mater. Proc. Technol.*, 1999, vols. 89–90, pp. 260-65.
33. J. Ye, B.Q. Han, F. Tang, and J.M. Schoenung: *Mater. Res. Soc. Symp. Proc.*, vol. 880E, pp. BB1.5.1, 2005.
34. J. Ye, B.Q. Han, Z. Lee, B. Ahn, S.R. Nutt, and J.M. Schoenung: *Scripta Mater.*, 2005, vol. 53, pp. 481-86.
35. J. He, J. Ye, E.J. Lavernia, D. Matejczyk, C. Bampton, and J.M. Schoenung: *J. Mater. Sci.*, 2004, vol. 39, pp. 6957-64.
36. H.P. Klug and L.E. Alexander: *X-ray Diffraction Procedures for Polycrystalline and Amorphous Materials*, John Wiley & Sons, New York, 1974, pp. 634-82.
37. L. Lü and M.O. Lai: *Mechanical Alloying*, Kluwer Academic Publishers, Boston, MA, 1998.
38. K.H. Chung, J. He, D.H. Shin, and J.M. Schoenung: *Mater. Sci. Eng., A*, 2003, vol. A356, pp. 23-31.
39. C.C. Koch: *Nanostruct. Mater.*, 1997, vol. 9, pp. 13-22.
40. K.H. Chung, J. Lee, R. Rodriguez, and E.J. Lavernia: *Metall. Mater. Trans. A*, 2002, vol. 33A, pp. 125-34.
41. R.F. Singer, W.C. Oliver, and W.D. Nix: *Metall. Trans. A*, 1980, vol. 11A, pp. 1895-901.
42. J. Ye, Z. Lee, B. Ahn, J. He, S.R. Nutt, and J.M. Schoenung: *Metall. Mater. Trans. A*, 2006, vol. 37A, pp. 3111-17.
43. X.F. Su, H.R. Chen, D. Kennedy, and F.W. Williams: *Composites*, 1999, vol. 30A, pp. 257-66.
44. G.P. Upit, S.A. Varchenya, and Y.E. Manik: *Automatic Welding Ussr.*, 1976, vol. 29, pp. 16-19.
45. V.V.B. Prasad, B.V.R. Bhat, Y.R. Mahajan, and P. Ramakrishnan: *Mater. Sci. Eng., A*, 2002, vol. A337, pp. 179-86.
46. H. Zhang, N. Maljkovic, and B.S. Mitchell: *Mater. Sci. Eng., A*, 2002, vol. A326, pp. 317-23.
47. S.L. Urtiga Filho, R. Rodriguez, J.C. Earthman, and E.J. Lavernia: *Mater. Sci. Forum, (Advanced Powder Technology III),* 2003, vols. 416–418, pp. 213-18.